ehp ENVIRONMENTAL HEALTH PERSPECTIVES
http://www.ehponline.org

Long-Term Trends Worldwide in Ambient NO_2 Concentrations Inferred from Satellite Observations

Jeffrey A. Geddes, Randall V. Martin, Brian L. Boys, and Aaron van Donkelaar

http://dx.doi.org/10.1289/ehp.1409567

Received: 6 December 2014
Accepted: 29 July 2015
Advance Publication: 4 August 2015

Environ Health Perspect DOI: 10.1289/ehp.1409567
Advance Publication: Not Copyedited

Long-Term Trends Worldwide in Ambient NO_2 Concentrations Inferred from Satellite Observations

Jeffrey A. Geddes,[1] Randall V. Martin,[1,2] Brian L. Boys,[1] and Aaron van Donkelaar[1]

[1]Department of Physics and Atmospheric Science, Dalhousie University, Halifax, Nova Scotia, Canada; [2]Harvard-Smithsonian Center for Astrophysics, Cambridge, Massachusetts, USA

Author correspondence to Jeffrey Geddes, Department of Physics and Atmospheric Science, Dalhousie University, Box 15000, Halifax, NS, B3H 4R2. E-mail: jeff.geddes@dal.ca

Running title: Satellite-derived trends in global ambient NO_2

Acknowledgments: We acknowledge the free use of tropospheric NO_2 column data from www.temis.nl. This work was supported by the Natural Science and Engineering Research Council (NSERC) of Canada and by Health Canada. Funding for Geddes was supported by NSERC CREATE IACPES (iacpes.info.york.ca).

Competing financial interests: The authors declare no competing financial interests.

Abstract

Background: Air pollution is associated with morbidity and premature mortality. Satellite remote sensing provides globally consistent decadal-scale observations of ambient NO_2 pollution.

Objective: We determined global population-weighted annual mean NO_2 concentrations from 1996 through 2012.

Methods: We used observations of NO_2 tropospheric column densities from three satellite instruments in combination with chemical transport modeling to produce a global 17-year record of ground-level NO_2 at 0.1° x 0.1° resolution. We calculated linear trends in population-weighted annual mean NO_2 (PWM_{NO2}) concentrations in different regions around the world as defined by the Global Burden of Disease Study.

Results: We found that PWM_{NO2} in High-Income North America (Canada and the U.S.) decreased more steeply than in any other region, having declined by -4.7% yr^{-1} (95% confidence interval (CI): -5.3, -4.1). PWM_{NO2} decreased in Western Europe at a rate of -2.5% yr^{-1} (95% CI: -3.0, -2.1). The highest PWM_{NO2} occurred in High-Income Asia Pacific (predominantly Japan and South Korea) in 1996, with a subsequent decrease of -2.1% yr^{-1} (95% CI: -2.7, -1.5). In contrast, PWM_{NO2} almost tripled in East Asia (China, North Korea, and Taiwan), at a rate of 6.7% yr^{-1} (95% CI: 6.0, 7.3). The satellite-derived estimates of trends in ground-level NO_2 were consistent with regional trends inferred with ground-station monitoring networks in North America (within 0.7% yr^{-1}) and Europe (within 0.3% yr^{-1}). Our rankings of regional average NO_2 and long-term trends differed from the satellite-derived estimates of fine particulate matter reported elsewhere, demonstrating the utility of both indicators to describe changing pollutant mixtures.

Conclusions: Long-term trends in satellite-derived ambient NO_2 provide new information about changing global exposure to ambient air pollution. Our estimates are publicly available at http://fizz.phys.dal.ca/~atmos/martin/?page_id=232.

Introduction

Globally, over three million premature deaths were attributed to ambient air quality in 2010 (Lim et al. 2012), and it has been estimated to cost the U.S. between $71 and $277 billion in gross annual damages primarily due to premature mortality and illness (Muller and Mendelsohn 2007). Decades of large cohort studies have established strong associations between air pollution and human mortality, with increasing evidence of a "no-threshold" model where adverse health effects can be recognised even at low ambient levels (Anderson 2009; World Health Organization 2006). As air quality around the world evolves, global observations of these long-term changes would offer valuable insight into trends in exposure.

Nitrogen dioxide (NO_2) is a major constituent of the air pollution mix. Strong associations between NO_2 and mortality have been identified in multi-city studies around the world (Burnett et al. 2004; MacIntyre et al. 2014; Samoli et al. 2006; Tao et al. 2012). There is inconsistent evidence for a mechanistic driver of the effect of NO_2 on health (Hesterberg et al. 2009), and thus it is unclear if NO_2 acts as an independent cause of mortality. Rather, there is consensus that NO_2 could act as a proxy or surrogate species either for constituents that are not being monitored, or more generally for the multi-pollutant mix (Brook et al. 2007; Brunekreef and Holgate 2002; Levy et al. 2014). NO_2 has consequently been included in multi-pollutant health indices (Stieb et al. 2008), and is strictly monitored in some regions (World Health Organization 2006).

Given the robustness of NO_2 as a predictor of the effects of air pollution on health there is strong interest in long-term estimates of historical concentrations, but few regions worldwide, especially in developing countries, have sufficient observations for exposure assessment. In a

few parts of the world ground-station monitoring networks have operated for decades, providing a valuable record to evaluate satellite-based trends in air pollution.

Seltenrich (2014) summarized the opportunities offered by remote sensing for environmental health research in a recent Focus article from *Environmental Health Perspectives*. Novotny et al. (2011), and Vienneau et al. (2013) have combined satellite data and land-use regression to calculate population-weighted mean NO_2 over the United States in 2006 and Western Europe in 2005-2007 respectively. Such data have found novel applications in exploring disparities in exposure by socioeconomic factors (Clark et al. 2014). Observations of tropospheric NO_2 vertical column densities from satellite instruments have provided evidence of dramatic changes over the United States (Duncan et al. 2013; Russell et al. 2012) and around the world (Hilboll et al. 2013; Richter et al. 2005; van der A et al. 2008). These results show the potential to document globally consistent changes in total atmospheric burden, but the observations have yet to be extended to long-term surface-level concentrations.

Here, we inferred annual mean ambient ground-level NO_2 concentrations worldwide from 1996 to 2012 using observations of NO_2 tropospheric column density from three satellite instruments together with a chemical transport model. We investigated trends in regional population-weighted mean NO_2 concentrations over these 17 years and contrasted our results with similar published estimates for $PM_{2.5}$.

Methods

Satellite observations

We used NO_2 column observations from the Global Ozone Monitoring Experiment (GOME), Scanning Imaging Absorption Spectrometer for Atmospheric Cartography (SCIAMACHY), and

GOME-2 satellite instruments. Information on these satellite instruments is available at https://earth.esa.int/. We chose these instruments for their similar observation times (typically 9:30-11:30 am, 9:00-11:00 am, and 8:30-10:30 am local time respectively), with some temporal overlap due to the range of viewing angles. Data were obtained from http://www.temis.nl/airpollution/ (TM4NO2A version 2.3). The NO_2 column densities are retrieved from measurements of backscattered sunlight (Boersma et al. 2004). The GOME instrument provided observations from 1995 to 2003, with a spatial resolution of 320km x 40km, and covering the globe roughly every 3 days. SCIAMACHY provided observations from 2002-2011, at 60km x 30km resolution with global coverage in about 6 days. GOME-2 continues to observe since 2007 with a spatial resolution of 80km x 40km, covering the world in a day. We regridded the daily data from each instrument to a regular 0.1°×0.1° grid worldwide. This approximately 10 km×10 km resolution is finer than any of the individual instruments, but allows for direct comparison between them. Detection of smoothed features at scales below instrument pixel dimensions can occur for long-term mean quantities due to spatial oversampling (Streets et al. 2013).

We excluded data contaminated by cloud or snow by rejecting bright pixels (cloud radiance fraction > 0.5), and filtering data according shortest snow-free season (estimated by marking the last day of snow cover and first day of snow arrival in each pixel every year, using data from the Interactive Snow and Ice Mapping System (http://dx.doi.org/10.7265/N52R3PMC)).

We accounted for the retrieval sensitivity by replacing the a priori NO_2 profile assumed in the retrieval using averaging kernels provided with the data, together with daily mean profiles

between 10:00-12:00 from a chemical transport model (GEOS-Chem) simulation, following Equation (1) of Lamsal et al. (2010).

Estimating ground-level NO_2

We used the GEOS-Chem model (Bey et al. 2001), version 9-01-03 (http://geos-chem.org), to simulate the relationship between satellite observations of tropospheric NO_2 column densities and the NO_2 concentrations at ground-level relevant to human exposure, following Lamsal et al. (2008, 2010). GEOS-Chem is a freely accessible community global chemical transport model that solves for time-varying three-dimensional atmospheric composition using equations that represent the chemistry and physics of the atmosphere. We conducted simulations for January 1996 to December 2012 at a horizontal resolution of 2° latitude by 2.5° longitude with 47 vertical levels (14 within the lowest 2 km), using assimilated meteorological fields (MERRA) provided by NASA's Global Modeling and Assimilation Office. Details of the simulations (e.g. emission inventories) are described in Boys et al. (2014).

Reconstructing consistent spatial resolution

The different horizontal resolution from the three satellite instruments has hindered the use of NO_2 satellite observations for long-term pollution studies. To derive a self-consistent record over the three instruments, one approach is to degrade higher resolution observations to a single consistent coarse resolution (e.g. van der A et al. (2008) and Konovalov et al. (2010)), but this forfeits the spatial information available from SCIAMACHY.

Here, we simulated fine spatial structure in both the GOME and GOME-2 observations by assuming that the relative spatial structure observed during the SCIAMACHY time period persists during the GOME and GOME-2 time periods. This approach exploits the general

persistence over multiple years of locations where NO_2 is produced. Similar approaches have been used for long-term trends in satellite observations of tropospheric NO_2 (Hilboll et al. 2013; Konovalov et al. 2008). We smoothed SCIAMACHY data using a two-dimensional box-car algorithm with an averaging window of 3.2° x 0.4°, roughly reflecting the horizontal smearing of the GOME resolution of 320km x 40km. We treated the smoothed SCIAMACHY data as a reproduction of GOME observations (global land-covered pixel-by-pixel scatter between mean SCIAMACHY and GOME was correlated with r=0.92 during their period of overlap from August 1, 2002 to June 30, 2003). We subsequently downscaled the annual mean GOME observations from 1996-2002 by applying the ratio of temporally averaged high-resolution (0.1° x 0.1°) observations in SCIAMACHY from 2003-2005 to the averaged smoothed (3.2° x 0.4°) observations. Figures S1A and S1B in the Supplemental Material show the results over North America for the year 1999. Urban centers smeared by GOME are resolved by SCIAMACHY.

This approach assumes that: (1) the relative spatial gradients of NO_2 do not change significantly over the GOME time period; and (2) the spatial gradients in NO_2 that were observed in 2003-2005 were representative of 1996-2002. We evaluated these assumptions during a period of rapid change in NO_2 columns (Supplemental Figure S1C and S1D): we smoothed the observations from 2009-2011 using the same 2-D box-car algorithm (Figure S1E), then downscaled the results using the high resolution observations from 2003-2005 (Figure S1F). The true observations from 2009-2011 (Figure S1D) were significantly correlated (r=0.97 over all land-covered pixels globally) with the simulated observations (Figure S1F). The correlations were also significant over specific domains where NO_2 columns have changed rapidly, including North America (r=0.96), Europe (r=0.96), and Asia (r=0.98).

We interpret these correlations as confirmation that our assumption of the general persistence in combustion source areas can plausibly be extended back during the GOME record. Although the resolutions of SCIAMACHY and GOME-2 are more similar, we found that a correction is still required to produce a self-consistent record. In this case, the reconstruction was based on a more direct comparison. The long-term ratio (2007-2011) of SCIAMACHY to GOME-2 was applied to each GOME-2 annual mean, with the assumption that scaling would be constant until 2012. The result is a self-consistent dataset at the effective resolution of SCIAMACHY for 1996-2012. After the spatial correction, we found significant agreement during overlapping periods between GOME and SCIAMACHY (r=0.89) and GOME-2 and SCIAMACHY (r=0.95). To further test for systematic evidence of a discontinuity or bias between sensor records, we calculated Z-scores for the difference in NO_2 between all neighboring years in the record of the individual pixels for major cities worldwide. The difference in NO_2 between 2003 (GOME) and 2004 (SCIAMACHY), and between 2011 (SCIAMACHY) and 2012 (GOME-2), were within 1.5 standard deviations for 94% of cases.

Evaluation using ground-based observations

We evaluated the satellite-derived product by comparing time series over ten densely-populated regions in North America and Europe with multiple continuous ground monitors from 1996-2012 within the surrounding ~200 km×200 km area. We focus on relative changes given the large spatial variation in absolute NO_2 concentrations within this area (Jerrett et al. 2007). We also evaluated our satellite-derived estimates of gridded NO_2 concentrations by comparing the long-term mean observations from the collocated ground-station monitors. Hourly observations of NO_2 across North America and Europe were from the U.S. Environmental Protection (http://www.epa.gov/ttn/airs/airsaqs/detaildata/downloadaqsdata.htm), Environment Canada

(http://maps-cartes.ec.gc.ca/rnspa-naps/data.aspx), and the European Environment Agency (http://www.eea.europa.eu/data-and-maps). The NO_2 recorded by these monitors is known to suffer from interferences of other reactive nitrogen compounds, resulting in a location-specific overestimate. Differences in representativeness between ground-station and satellite data also arise from comparing a point measurement with an area average, magnified by the tendency for ground monitors to be in locations with elevated NO_2 concentrations. We therefore focus on evaluating relative trends.

We calculated mid-morning (10:00-12:00) average observations each day. We excluded European stations identified as "traffic" to maximize site representativeness at the 0.1°x0.1° scale (no such identifier is available for the North American networks), but otherwise retained all rural, suburban, and urban locations (represented roughly equally). We required stations to have at least 5 satellite-coincident observations per year and at least 15 years of observations. Observations from multiple stations within a single pixel were averaged. We used completely sampled ground-based annual averages to evaluate the satellite-derived record.

Annual means and long-term trends

Incomplete sampling from the satellite instruments may introduce biases in long-term averages where NO_2 concentrations are correlated with season or cloudiness. We accounted for this by using a pixel-dependent correction, calculated as the annual ratio of GEOS-Chem simulated surface NO_2 sampled each day versus only on days with successful satellite retrievals. This approach has been used previously for NO_2 (Nowlan et al. 2014) and $PM_{2.5}$ (van Donkelaar et al. 2010) analyses.

We calculated long-term trends in annual means by ordinary least-squares linear regression, with 95% confidence intervals to establish uncertainty in the slopes. We use $\alpha = 0.01$ to test for statistical significance. We reported trends in % yr^{-1} relative to the long-term mean. We compared concentrations and trends in NO_2 with previously published values for $PM_{2.5}$.

Population data

We obtained worldwide gridded population counts (available at 5-year intervals from 1995-2015, with 2.5 arc minute resolution), from the NASA Socioeconomic Data and Applications Center (GPW v3, http://sedac.ciesin.columbia.edu/). We aggregated the data to 0.1° x 0.1° and linearly interpolated between each interval. We used these to calculate timeseries in population-weighted annual mean NO_2 (PWM_{NO2}) for the same regions used by the Global Burden of Disease Study 2010 (Lim et al. 2012; http://www.healthdata.org/gbd/).

Results

Figure 1 shows the satellite-derived long-term means and trends in ground-level NO_2 worldwide. We have made these data publicly available at http://fizz.phys.dal.ca/~atmos/martin/?page_id=232 ("Surface NO_2"). The most notable reductions were observed in North America, Western Europe, and Japan. In contrast, ground-level NO_2 substantially increased in East Asia and in isolated urban regions of the Middle East, Russia, and India. Trends for specific urban areas around the world are clearly distinguishable. For example, the steep increase isolated in northwestern China is around the city of Ürümqi (43.8°N, 87.6°E), where NO_2 increased at a rate of 10.1% yr^{-1} (95% CI: 8.0, 12.1).

The satellite-derived product was significantly correlated in space with the coincidently sampled ground-station observations in North America (r=0.80, N=223). The correlation was slightly

weaker across rural locations (r=0.72, N=41) than across non-rural locations (r=0.81, N=181). For Europe, we found the satellite-derived product was less strongly correlated with ground-station observations (r=0.57, N=365), but in this case rural locations were highly correlated (r=0.81, N=120), and non-rural locations less so (r=0.60, N=245). These correlations are consistent with previous comparisons of satellite NO_2 with monitoring networks (Blond et al. 2007; Lamsal et al. 2008; Lamsal et al. 2010). We attribute variation between rural and non-rural stations to differences in spatial representativeness of the sites, with urban monitors influenced by local pollution (e.g. traffic).

Figure 2 shows timeseries of spatially averaged annual mean ground-level NO_2 normalized to the long-term mean over ten urban areas with continuous observations. The majority of the trends in satellite-derived and ground-based mean NO_2 agree within the 95% confidence intervals. The last two panels of Figure 2 show satellite-derived NO_2 timeseries averaged over all North American (N=142) and European (N=305) pixels with continuous ground-station measurements, compared with mean ground-station measurements. The linear trends for the satellite estimates across North America of -4.4% yr^{-1} (95% CI: -5.0, -3.8) and across Europe of -2.2% yr^{-1} (95% CI: -2.8, -1.6) are consistent with ground-based measurement trends of -3.7% yr^{-1} (95% CI: -4.3, -3.2) and -1.9% yr^{-1} (95% CI: -2.3, -1.6).

Population-weighted annual mean NO_2

To our knowledge, this is the first data set that allows estimates of long-term global changes in area-wide ambient NO_2 concentrations relevant to outdoor exposure. Table 1 summarizes the long-term means and long-term trends in global and regional population-weighted annual mean NO_2 (PWM_{NO2}). Approximately 1.6 billion people lived in regions where average NO_2

significantly decreased ($p < 0.01$). In contrast, 3.2 billion people lived in regions where average NO_2 significantly increased ($p < 0.01$). The globally averaged PWM_{NO2} increased by 0.9% yr^{-1} (95% CI: 1.1, 0.6). The four regions with the highest long-term mean PWM_{NO2} are High Income Asia Pacific (Japan, South Korea, Brunei, and Singapore), Western Europe, High Income North America (Canada and the U.S.), and East Asia (China, North Korea, and Taiwan). All have trends significant to $p < 0.01$.

Figure 3 shows the 17-year annual PWM_{NO2} timeseries in these four regions, and maps of satellite-derived NO_2 concentrations at the beginning and end of the record. In Canada and the U.S. (Figure 3A and B), the satellite-derived estimates of PWM_{NO2} decreased by 50% overall, with a linear trend of -4.7% yr^{-1} (95% CI: -5.3, -4.1) relative to the long-term mean. The steepest decline occurred between 2004 and 2010, when PWM_{NO2} decreased at a rate of -7.0% yr^{-1} (95% CI: -5.8, -8.1) relative to the long term mean. This is statistically different from ($p < 0.01$), and almost three times steeper than, the trend of -2.5% yr^{-1} (95% CI: -4.0, -1.1) for earlier years between 1996 and 2003. The maps of NO_2 concentrations in North America demonstrate that the decreases were most notable over urban areas of the eastern United States and California.

The satellite-derived estimates of PWM_{NO2} in Western Europe (Figure 3C and D) also decreased between 1996 and 2012, declining 30% overall, with a linear trend of 2.5% yr^{-1} (95% CI: -3.0, -2.1). The trend from 1996 to 2003 (-2.9% yr^{-1}, 95% CI: -5.0, -1.0) was similar to that observed in North America over the same time. However, from 2004 to 2010 the decline in NO_2 in Western Europe (-2.0% yr^{-1}, 95% CI: -3.9, -0.2) was weaker than in North America (-7.0% yr^{-1}, 95% CI: -5.8, -8.1). The maps demonstrate notable decreases over the southern U.K., northern France, Germany, and Be-Ne-Lux regions.

The maps in Figures 3E and F encompass both the East Asia and High Income Asia Pacific regions. Before 2010, the highest PWM_{NO2} of all GBD regions was consistently observed for Asia Pacific (South Korea and Japan account for 97% of this population). The region experienced a decrease of 20% from 1996 levels, with a linear trend of -2.1% yr^{-1} (95% CI: -2.7, -1.5). In contrast, our satellite-derived ground-level estimates indicate that PWM_{NO2} in East Asia increased 2.7 times over the same period of time, at a rate of 6.7% yr^{-1} (95% CI: 6.0, 7.3) and now has the highest PWM_{NO2} of all GBD regions. China accounts for 97% of this population, and the maps in Figure 3E and F show the notable increase in NO_2 for eastern China in particular.

The GPW population distribution changed remarkably across East Asia from 1996 to 2012. However, the increase in region-wide PWM_{NO2} was dominated almost entirely by changes in NO_2 as opposed to changes in population. If the population is held constant at 1996 levels, the trend in PWM is 6.5% yr^{-1} (95% CI: 5.9, 7.1), well within the 95% confidence interval of the original slope. Likewise, the slopes for Western Europe, North America, and Asia Pacific were within the original 95% confidence intervals when population changes were ignored (data not shown).

Distribution of population and NO_2

Figure 4 further investigates the population-weighted changes in ambient NO_2 as cumulative distribution plots for the same four regions depicted in Figure 3. The most extreme ambient concentrations changed locations over time, moving from North America and Western Europe in 1996 to East Asia by 2012.

In North America (Figure 4A), the 99th percentile of the population-weighted ambient NO_2 concentration (highest exposure) decreased by 42% (from 15.7 to 9.0 ppb), and the 50th percentile decreased by 54% (from 3.8 to 1.7 ppb). Concentrations even decreased for less exposed populations, with the lowest 10th percentile also decreasing by about 50% (from 1.1 ppb to 0.6 ppb).

In Western Europe (Figure 4B), the 99th and 50th percentiles of the population-weighted ambient NO_2 concentration both decreased by about 30% (from 12.9 to 9.1 ppb and 4.1 to 2.9 ppb respectively). In contrast, the lowest 10th percentile only decreased by about 10% (from 1.0 ppb to 0.9 ppb).

In Asia Pacific (Figure 4C), improvements were similarly modest across all segments of the population. The 99th and 50th percentile of the population-weighted ambient NO_2 concentration decreased by 16% (from 15.9 to 13.4 ppb) and 12% (4.1 to 3.6 ppb) respectively. The cleanest 10th percentile decreased by 24% (from 0.8 ppb to 0.6 ppb).

In contrast to the other three regions highlighted, NO_2 concentrations have increased for more than 90% of the population in East Asia (Figure 4D). The 99th percentile of the population-weighted ambient NO_2 concentration more than doubled between 1996 and 2012 (from 8.9 ppb to 21.6 ppb). Likewise, the 50th percentile tripled (from 1.0 to 2.9 ppb). The 10th percentile also doubled (from 0.3 to 0.6 ppb), illustrating that conditions deteriorated for the less exposed segments of the population as well.

Comparing global ground-level NO_2 and $PM_{2.5}$ distributions

Comparison of NO_2 and fine particulate matter ($PM_{2.5}$) offers insight into the air pollution mixture, and the sources affecting exposure. Table 2 contains satellite-derived estimates of

population-weighted $PM_{2.5}$ trends and long-term mean concentrations from van Donkelaar et al. (2014) for the same regions used here, and our results for NO_2 for the same time period (1998-2012).

East Asia has the highest long-term population-weighted concentrations of $PM_{2.5}$ (50.3 $\mu g/m^{-3}$, Table 2) but ranks fourth for NO_2 (3.3 ppb). On the other hand, while Asia Pacific ranks highest in terms of NO_2 (4.7 ppb), it ranks seventh for $PM_{2.5}$ (16.8 $\mu g/m^{-3}$). South Asia experienced the second highest ambient concentrations of $PM_{2.5}$ (34.6 $\mu g/m^{-3}$), yet only ranks fifteenth for NO_2 (0.5 ppb). Another significant shift in ranking occurs for North America, whose population was exposed to the world's third highest ambient concentrations of NO_2 (3.5 ppb) but is ranked much lower (twelfth) in terms of $PM_{2.5}$ (9.9 $\mu g/m^{-3}$).

Table 2 shows that of all the GBD regions, North America had the steepest declines in both NO_2 (-5.3% yr^{-1}, 95% CI: -6.0, -4.6) and $PM_{2.5}$ (-3.3% yr^{-1}, 95% CI: -4.1, -2.5) ambient concentrations. The only other region with statistically significant declines in both was Western Europe. Of the remaining seven regions with significant decreasing trends NO_2, none had significant changes in $PM_{2.5}$; most notably this occurred in Asia Pacific. On the other hand, $PM_{2.5}$ significantly increased in eight regions but only three of these had significant increases in NO_2 as well (East Asia, North Africa / Middle East, and South Asia). Southern Sub-saharan Africa is the only region where statistically significant trends were in opposing directions (decreasing NO_2, increasing $PM_{2.5}$).

Uncertainty in the satellite-derived trends

We used the comparison with ground-station observations across North America and Europe to assess the error in our regional satellite-derived trends. The confidence intervals of the satellite-

derived trends (± 0.6% yr^{-1} over North America and Europe from the last two panels of Figure 2) roughly describe the difference between the satellite-derived and in-situ trends (0.7% yr^{-1} for North America, 0.3% yr^{-1} for Europe). Thus we treat the confidence intervals as a proxy measure of error in the relative trends where ground-based observations do not exist. The steeper slope derived from the regional averaged satellite observations compared to ground-based measurements (last two panels of Figure 2) implies there could be a small systematic bias in the satellite-derived trends, but this may be attributable to representativeness differences in the observed quantities (spatial average from the satellite vs. point measurements by the ground monitors).

Sampling losses in the satellite record due to quality control filtering contribute to systematic error in annual mean. For 13 of the 21 regions, our correction for incomplete sampling changes the calculated PWM_{NO2} by less than 25%. However, in the northern latitudes with seasonal snow cover, the correction term becomes large due to the seasonality of NO_2 concentrations. The correction is largest for Western Europe and increases long-term PWM_{NO2} by 60% (from 2.6 ppb to 4.1 ppb). Globally, the correction increases PWM_{NO2} by 33% (from 1.2 ppb to 1.6 ppb). However, these errors insignificantly impact the reported relative trends for the GBD regions.

We tested the sampling correction by comparing the linear regression slopes with and without adjusting for sampling bias. In all cases, the sampling correction had statistically insignificant impact on the regional trends in PWM_{NO2}. For example, the trend over North America without the sampling correction was -4.7% yr^{-1} (95% CI: -5.5, -3.9), vs. -4.7% yr^{-1} (95% CI: -5.3, -4.1) with the correction. Likewise in Western Europe, where the correction was largest, the trend was -2.4% yr^{-1} (95% CI: -3.3, -1.4), vs. -2.5% yr^{-1} (95% CI: -3.0, -2.1) with the correction. Globally,

the trend without the sampling correction was 1.3% yr^{-1} (95% CI: 0.9, 1.6), vs. 0.9% yr^{-1} (95% CI: 0.6, 1.1) with the correction ($p = 0.04$).

While other systematic errors in annual mean NO_2 are expected to have less influence on the trend calculation, and estimating trends over large regions reduces random error across space, we caution that errors in annual NO_2 over any individual 0.1° x 0.1° pixel will be larger. Error in estimating ground-level NO_2 from satellite observations (due to errors in the simulated profile and in the retrieved column densities) has been previously estimated as -11% to +36% (Lamsal et al. 2008). Error introduced by simulating spatial resolution in the GOME and GOME-2 observations could also be large over an individual pixel, although in the comparison with ground-based observations over large samples, we found no perceptible bias resulting from our approach. Given this evidence, we expect the latter error is random and mitigated by spatial averaging.

Discussion

NO_2 acts as an indicator for exposure to unmeasured toxics in the air pollution mix (Brook et al. 2007), and continues to have strong associations with negative health outcomes (MacIntyre et al. 2014). However, traditional ground-station NO_2 monitoring networks have poor spatial coverage, resulting in large gaps in assessments of human exposure (Guay et al. 2011), especially in developing countries. We found that satellite observations can be used to derive global long-term changes in ambient NO_2 concentrations at spatial scales relevant for average human exposure (0.1° x 0.1°). The record offers almost complete spatial coverage, not only supplementing gaps in established ground-station observing networks, but also providing insight over regions without prior observations.

Using our satellite-derived ground-level NO_2 concentrations, we calculated trends in population-weighted annual mean NO_2 worldwide from 1996-2012. Decreasing trends were found in North America (-4.7% yr^{-1}), Western Europe (-2.5% yr^{-1}), and Asia Pacific (-2.1% yr^{-1}). Increasing trends were found in East Asia (6.7% yr^{-1}), North Africa / Middle East (2.4% yr^{-1}), and South Asia (1.3% yr^{-1}). The trend in global PWM_{NO2} was increasing (0.9% yr^{-1}), and statistically significant. Our trends in PWM_{NO2} were consistent with ground-based measurements in North America and Europe, and with previous work describing changes in NO_2 tropospheric columns over North America (e.g. Duncan et al. 2013, Russell et al. 2012), China (Mijling et al. 2013; Richter et al. 2005), and over the megacity regions studied in Hilboll et al. 2013. Our satellite-derived timeseries is freely available as a public good (http://fizz.phys.dal.ca/~atmos/martin/?page_id=232).

The regional trends reflected differing trajectories of anthropogenic activities and policies around the world. For example, increases in PWM_{NO2} for East Asia and for the Middle East from 1996-2012 reflect rapid development in regions where emissions have been rising but remain uncertain (e.g. Zhang et al. 2007). On the other hand, the modest decline in PWM_{NO2} in North America between 1996 and 2003, followed by steeper decreases post-2004 might arise from the U.S. EPA "NO_x State implementation Plans". These plans required NO_x emission reduction measures by mid-2003, and total anthropogenic emissions in the U.S. decreased by 26% between 2004 and 2009 (Environmental Protection Agency 2014). The steeper decline in PWM_{NO2} during this time (40%) compared to the reported emissions from the EPA and to the decrease in area-weighted mean NO_2 (25%, not shown), suggests that emission reductions successfully and most efficiently targeted air quality in populated regions. Other factors, including the 2008 economic recession (Castellanos and Boersma 2012; Russell et al. 2012), may have also played a role.

The regional rankings of population weighted NO_2 concentrations, and the long-term trends, differed from previously reported values for $PM_{2.5}$ (van Donkelaar et al. 2014), suggesting that these observations provide complementary information on the changing global air pollution mixture. For example, some regions that ranked highest in terms of $PM_{2.5}$ (e.g. East Asia and South Asia) ranked lower for NO_2. A driver of these differences is the type of combustion that produces NO_2 and $PM_{2.5}$, with biofuel sources in South Asia and intense coal burning in East Asia (Lu et al. 2011). We also found regions where NO_2 significantly declined while $PM_{2.5}$ was not significantly different (e.g. Asia Pacific). Comparison of epidemiologic studies for the various regions could yield insight into the health effects of different pollution source types.

Caution must be taken in comparing the satellite-derived ground-level NO_2 concentrations we obtained to the WHO air quality guideline for NO_2. NO_2 exhibits dramatic within-city spatial variation (Jerrett et al. 2005; Wang et al. 2014), which this satellite-derived data cannot fully resolve. For example, this data set is not appropriate for determining gradients in exposure near roadways. Plumes from stack emissions could result in additional errors. Our estimates represent area-averages (~10 km×10 km), while the WHO guideline was established for point measurements that are often not representative of area averages. We hypothesize that the area-averaged record from satellites represents what a randomly distributed monitoring network would obtain, potentially mitigating systematic biases in studies of exposure that result from station placement and poor network coverage (Goldman et al. 2010; Sheppard et al. 2012). We have focused on long (annual) averaging times to minimize the daily variability in the relationship between column-to-surface concentrations (Knepp et al. 2013) that may not be fully captured by the chemical transport model. These data are therefore also better suited to long-term than short term studies.

We reported trends in population-weighted averages to assess changes in NO_2 around the world, selecting regions according to the Global Burden of Disease Study for a convenient grouping of nations based on "geographic closeness and epidemiological similarities" (www.healthdata.org/gbd/faq). These regional population-weighted averages are indirectly related to average human exposure. Personal exposure would need to account for additional factors such as individual activity patterns and indoor versus outdoor contributions.

Multiple opportunities are anticipated for further development. We expect improvements in this approach from the increasing resolution of future satellite NO_2 observations and from higher resolution modeling of the relationship between ground-level concentrations and the observed column densities. Land use regression could offer additional valuable fine-scale information (Novotny et al. 2011; Vienneau et al. 2013). Forthcoming geostationary platforms dedicated to air quality (e.g. TEMPO (http://science.nasa.gov/missions/tempo/), Sentinel-4 (https://sentinel.esa.int/web/sentinel/missions/sentinel-4), and GEMS (Lasnik et al. 2014)) will also significantly increase temporal coverage. Our results add complementary information to the assessment of population exposure to air pollution.

References

Anderson HR. 2009. Air pollution and mortality: A history. Atmos. Environ. 43:142–152; doi:10.1016/j.atmosenv.2008.09.026.

Bey I, Jacob DJ, Yantosca RM, Logan JA, Field BD, Fiore AM, et al. 2001. Global modeling of tropospheric chemistry with assimilated meteorology: Model description and evaluation. J. Geophys. Res. 106:23073; doi:10.1029/2001JD000807.

Boersma KF, Eskes HJ, Brinksma EJ. 2004. Error analysis for tropospheric NO2 retrieval from space. J. Geophys. Res. 109:D04311–D04311; doi:10.1029/2003JD003962.

Boys BL, Martin RV, van Donkelaar A, Macdonell RJ, Hsu NC, Cooper, M, et al. 2014. Fifteen-year global time series of satellite-derived fine particulate matter. Environ. Sci. Technol. doi:10.1021/es502113.

Blond N, Boersma KF, Eskes HJ, van der A RJ, Van Roozendael M, De Smedt I, et al. 2007. Intercomparison of SCIAMACHY nitrogen dioxide observations, in situ measurements and air quality modeling results over Western Europe. J. Geophys. Res. 112, doi:10.1029/2006JD007277.

Brook JR, Burnett RT, Dann TF, Cakmak S, Goldberg MS, Fan X, et al. 2007. Further interpretation of the acute effect of nitrogen dioxide observed in Canadian time-series studies. J. Expo. Sci. Environ. Epidemiol. 17 Suppl 2:S36–44; doi:10.1038/sj.jes.7500626.

Brunekreef B, Holgate ST. 2002. Air pollution and health. Lancet 360: 1233–1242.

Burnett RT, Stieb D, Brook JR, Cakmak S, Dales R, Raizenne M, et al. 2004. Associations between short-term changes in nitrogen dioxide and mortality in Canadian cities. Arch. Environ. Health 59:228–36; doi:10.3200/AEOH.59.5.228-236.

Castellanos P, Boersma KF. 2012. Reductions in nitrogen oxides over Europe driven by environmental policy and economic recession. Scientific Reports. 2:265; doi:10.1038/srep00265.

Clark LP, Millet DB, Marshall JD. 2014. National patterns in environmental injustice and inequality: outdoor NO2 air pollution in the United States. PLoS One 9:e94431; doi:10.1371/journal.pone.0094431.

Duncan BN, Yoshida Y, de Foy B, Lamsal LN, Streets DG, Lu Z, et al. 2013. The observed response of Ozone Monitoring Instrument (OMI) NO2 columns to NOx emission controls on power plants in the United States: 2005–2011. Atmos. Environ. 81:102–111; doi:10.1016/j.atmosenv.2013.08.068.

Environmental Protection Agency. 2014. National Emissions Inventory (NEI) Air Pollutant Emissions Trends Data, Updated February 2014. Technol. Transf. Netw. Clear. Invent. Emiss. Factors. Available: http://www.epa.gov/ttn/chief/trends/index.html [accessed 30 October 2014].

Goldman GT, Mulholland JA, Russell AG, Srivastava A, Strickland MJ, Klein M, et al. 2010. Ambient air pollutant measurement error: characterization and impacts in a time-series epidemiologic study in Atlanta. Environ. Sci. Technol. 44:7692–8; doi:10.1021/es101386r.

Guay M, Stieb DM, Smith-Doiron M. 2011. Assessment of long-term exposure to air pollution in a longitudinal national health survey. J. Expo. Sci. Environ. Epidemiol. 21:337–42; doi:10.1038/jes.2010.37.

Hesterberg TW, Bunn WB, McClellan RO, Hamade AK, Long CM, Valberg PA. 2009. Critical review of the human data on short-term nitrogen dioxide (NO2) exposures: evidence for NO2 no-effect levels. Crit. Rev. Toxicol. 39:743–81; doi:10.3109/10408440903294945.

Hilboll A, Richter A, Burrows JP. 2013. Long-term changes of tropospheric NO_2 over megacities derived from multiple satellite instruments. Atmos. Chem. Phys. 13:4145–4169; doi:10.5194/acp-13-4145-2013.

Jerrett M, Arain A, Kanaroglou P, Beckerman B, Potoglou D, Sahsuvaroglu T, et al. 2005. A review and evaluation of intraurban air pollution exposure models. J. Expo. Anal. Environ. Epidemiol. 15:185–204; doi:10.1038/sj.jea.7500388.

Jerrett M, Arain MA, Kanaroglou P, Beckerman B, Crouse D, Gilbert NL, et al. 2007. Modeling the intraurban variability of ambient traffic pollution in Toronto, Canada. J. Toxicol. Environ. Health. A 70:200–12; doi:10.1080/15287390600883018.

Knepp T, Pippin M, Crawford J, Chen G, Szykman J, Long R, Estimating surface NO2 and SO2 mixing ratios from fast-response total column observations and potential application to geostationary missions. J. Atmos. Chem. doi:10.1007/s10874-013-9257-6.

Konovalov IB, Beekmann M, Burrows JP, Richter A. 2008. Satellite measurement based estimates of decadal changes in European nitrogen oxides emissions. Atmos. Chem. Phys. 8:2623–2641; doi:10.5194/acp-8-2623-2008.

Konovalov IB, Beekmann M, Richter A, Burrows JP, Hilboll A. 2010. Multi-annual changes of NO_x emissions in megacity regions: nonlinear trend analysis of satellite measurement based estimates. Atmos. Chem. Phys. 10:8481–8498; doi:10.5194/acp-10-8481-2010.

Lamsal LN, Martin R V, van Donkelaar A, Steinbacher M, Celarier EA, Bucsela E, et al. 2008. Ground-level nitrogen dioxide concentrations inferred from the satellite-borne Ozone Monitoring Instrument. J. Geophys. Res. D Atmos. 113: D16308.

Lamsal LN, Martin R V., van Donkelaar A, Celarier EA, Bucsela EJ, Boersma KF, et al. 2010. Indirect validation of tropospheric nitrogen dioxide retrieved from the OMI satellite instrument: Insight into the seasonal variation of nitrogen oxides at northern midlatitudes. J. Geophys. Res. 115:D05302; doi:10.1029/2009JD013351.

Lasnik J, Stephens M, Baker B, Randall C, Ko DH, Kim S, et al. 2014. Geostationary Environment Monitoring Spectrometer (GEMS) over the Korea peninsula and Asia-Pacific region. Abstract A51A-3003 presented at 2014 Fall Meeting, AGU, San Francisco, Calif., 15-19 Dec.

Levy I, Mihele C, Lu G, Narayan J, Brook JR. 2014. Evaluating multipollutant exposure and urban air quality: pollutant interrelationships, neighborhood variability, and nitrogen dioxide as a proxy pollutant. Environ. Health Perspect. 122:65–72; doi:10.1289/ehp.1306518.

Lim SS, Vos T, Flaxman AD, Danaei G, Shibuya K, Adair-Rohani H, et al. 2012. A comparative risk assessment of burden of disease and injury attributable to 67 risk factors and risk factor clusters in 21 regions, 1990-2010: a systematic analysis for the Global Burden of Disease Study 2010. Lancet 380:2224–60; doi:10.1016/S0140-6736(12)61766-8.

Lu Z, Zhang Q, Streets DG. 2011. Sulfur dioxide and primary carbonaceous aerosol emissions in China and India, 1996–2010. Atmos. Chem. Phys. 11:9839–9864; doi:10.5194/acp-11-9839-2011.

MacIntyre EA, Gehring U, Mölter A, Fuertes E, Klümper C, Krämer U, et al. 2014. Air pollution and respiratory infections during early childhood: an analysis of 10 European birth cohorts within the ESCAPE Project. Environ. Health Perspect. 122:107–13; doi:10.1289/ehp.1306755.

Mijling B, van der A RJ, Zhang Q. 2013. Regional nitrogen oxides emission trends in East Asia observed from space. Atmos. Chem. Phys. 13:12003–12012; doi:10.5194/acp-13-12003-2013.

Muller NZ, Mendelsohn R. 2007. Measuring the damages of air pollution in the United States. J. Environ. Econ. Manage. 54:1–14; doi:10.1016/j.jeem.2006.12.002.

Novotny E V, Bechle MJ, Millet DB, Marshall JD. 2011. National satellite-based land-use regression: NO2 in the United States. Environ. Sci. Technol. 45:4407–14; doi:10.1021/es103578x.

Nowlan CR, Martin R V., Philip S, Lamsal LN, Krotkov NA, Marais EA, et al. 2014. Global dry deposition of nitrogen dioxide and sulfur dioxide inferred from space-based measurements. Global Biogeochem. Cycles n/a–n/a; doi:10.1002/2014GB004805.

Richter A, Burrows JP, Nüss H, Granier C, Niemeier U. 2005. Increase in tropospheric nitrogen dioxide over China observed from space. Nature 437:129–32; doi:10.1038/nature04092.

Russell AR, Valin LC, Cohen RC. 2012. Trends in OMI NO_2 observations over the United States: effects of emission control technology and the economic recession. Atmos. Chem. Phys. 12:12197–12209; doi:10.5194/acp-12-12197-2012.

Samoli E, Aga E, Touloumi G, Nisiotis K, Forsberg B, Lefranc A, et al. 2006. Short-term effects of nitrogen dioxide on mortality: an analysis within the APHEA project. Eur. Respir. J. 27:1129–38; doi:10.1183/09031936.06.00143905.

Seltenrich N. 2014. Remote-sensing applications for environmental health research. Environ. Health Perspect. 122:A268–75; doi:10.1289/ehp.122-A268.

Sheppard L, Burnett RT, Szpiro AA, Kim S-Y, Jerrett M, Pope CA, et al. 2012. Confounding and exposure measurement error in air pollution epidemiology. Air Qual. Atmos. Health 5:203–216; doi:10.1007/s11869-011-0140-9.

Stieb DM, Burnett RT, Smith-Doiron M, Brion O, Shin HH, Economou V. 2008. A new multipollutant, no-threshold air quality health index based on short-term associations observed in daily time-series analyses. J. Air Waste Manag. Assoc. 58: 435–50.

Streets DG, Canty T, Carmichael GR, de Foy B, Dickerson RR, Duncan BN, et al 2013. Emissions estimation from satellite retrievals: A review of current capability. Atmos. Env. 77: 1011-1042.

Tao Y, Huang W, Huang X, Zhong L, Lu S-E, Li Y, et al. 2012. Estimated acute effects of ambient ozone and nitrogen dioxide on mortality in the Pearl River Delta of southern China. Environ. Health Perspect. 120:393–8; doi:10.1289/ehp.1103715.

van der A RJ, Eskes HJ, Boersma KF, van Noije TPC, Van Roozendael M, De Smedt I, et al. 2008. Trends, seasonal variability and dominant NO x source derived from a ten year record of NO 2 measured from space. J. Geophys. Res. 113:D04302; doi:10.1029/2007JD009021.

van Donkelaar A, Martin R V, Brauer M, Kahn R, Levy R, Verduzco C, et al. 2010. Global estimates of ambient fine particulate matter concentrations from satellite-based aerosol optical depth: Development and application. Environ. Health Perspect. 118: 847–855.

van Donkelaar A, Martin R V., Brauer M, Boys B. 2014. Use of satellite observations for long-term exposure assessment of global concentrations of fine particulate matter. Environ. Health Perspect. DOI:10.128.

Vienneau D, de Hoogh K, Bechle MJ, Beelen R, van Donkelaar A, Martin R V, et al. 2013. Western European land use regression incorporating satellite- and ground-based measurements of NO2 and PM10. Environ. Sci. Technol. 47:13555–64; doi:10.1021/es403089q.

Wang M, Beelen R, Bellander T, Birk M, Cesaroni G, Cirach M, et al. 2014. Performance of multi-city land use regression models for nitrogen dioxide and fine particles. Environ. Health Perspect. 122:843–9; doi:10.1289/ehp.1307271.

World Health Organization. 2006. *WHO Air quality guidelines for particulate matter, ozone, nitrogen dioxide and sulfur dioxide - Global update 2005 - Summary of risk assessment*. WHO Press, Geneva.

Zhang Q, Streets DG, He K, Wang Y, Richter A, Burrows JP, et al. 2007. NO x emission trends for China, 1995–2004: The view from the ground and the view from space. J. Geophys. Res. 112:D22306; doi:10.1029/2007JD008684.

Table 1: Satellite-derived population-weighted mean NO_2 concentrations, linear trends from 1996-2012, and population within Global Burden of Disease regions[a]. Results are in descending order of mean NO_2.

Region	Mean (1996-2012) NO_2[ppb]	Trend [% yr^{-1}] (95% C.I.)	P-value	Population [million people]
1. Asia Pacific (High Income)	4.9	-2.1(-2.7,-1.5)	< 0.01	176
2. Western Europe	4.1	-2.5(-3.0,-2.1)	< 0.01	399
3. North America (High Income)	3.7	-4.7(-5.3,-4.1)	< 0.01	329
4. East Asia	2.9	6.7(6.0,7.3)	< 0.01	1351
5. Eastern Europe	2.2	1.4(0.0,2.9)	0.05	212
6. Central Europe	2.1	-1.4(-2.1,-0.7)	< 0.01	121
7. Southern Latin America	1.3	-1.0(-2.4, 0.3)	0.12	59
8. Central Latin America	1.0	-2.0(-3.0,-1.0)	< 0.01	218
9. Australasia	0.9	-1.5(-2.2,-0.8)	< 0.01	23
10. Southern Sub-saharan Africa	0.9	-1.2(-1.8,-0.5)	< 0.01	65
11. North Africa / Middle East	0.7	2.4(1.8,3.1)	< 0.01	411
12. Tropical Latin America	0.7	-2.6(-3.6,-1.6)	< 0.01	189
13. Central Asia	0.6	0.3(-1.4,1.9)	0.30	79
14. Andean Latin America	0.6	0.5(-0.5,1.4)	0.71	51
15. South Asia	0.5	1.3(0.4,2.2)	< 0.01	1455
16. Southeast Asia	0.5	0.0(-0.7,0.7)	0.96	578
17. Caribbean	0.2	-1.1(-2.2,0.0)	0.05	25
18. West Sub-saharan Africa	0.2	-0.2(-1.1,0.6)	0.56	282
19. Central Sub-saharan Africa	0.1	-1.3(-2.1,-0.6)	< 0.01	85
20. East Sub-saharan Africa	0.1	-0.1(-0.9,0.6)	0.70	301
21. Oceania	< 0.1	-2.9(-5.4,-0.5)	0.02	7
GLOBAL	**1.6**	**0.9(0.6,1.1)**		**6357**

[a]Lim et al. (2012)

Table 2: Long-term means and trends in satellite-derived population-weighted ground-level mean NO_2 compared with long-term means and trends in satellite-derived population-weighted $PM_{2.5}$ from van Donkelaar et al. 2014. Numbers in parenthesis for mean $PM_{2.5}$ give regional ranking.

Region	**Mean (2001-2010) NO_2[ppb]**	**1998-2012 trend in NO_2 [% yr^{-1}] (95% C.I.)**	**2001-2010 $PM_{2.5}$[μg m^{-3}] (ranking)**	**1998-2012 trend in $PM_{2.5}$ [% yr^{-1}] (95% C.I.)**
Asia Pacific (High Income)	4.7	-2.1(-2.9,-1.3)	16.8(7)	-0.4(-1.2,0.4)
Western Europe	3.9	-2.3(-2.9,-1.8)	13.5(8)	-1.9(-2.8,-1.0)
North America (High Income)	3.5	-5.3(-6.0,-4.6)	9.9(12)	-3.3(-4.1,-2.5)
East Asia	3.3	6.5(5.8,7.3)	50.3(1)	3.2(2.1,4.3)
Eastern Europe	2.3	1.8(-0.1,3.6)	12.6(9)	-0.3(-2.0,1.4)
Central Europe	2.0	-0.8(-1.6,-0.1)	17.8(5)	-1.2(-2.7,0.3)
Southern Latin America	1.3	-0.6(-2.3,1.1)	6.4(17)	1.3(-0.1,2.7)
Central Latin America	1.0	-2.2(-3.3,-1.1)	8.5(14)	-0.8(-1.6,0)
Australasia	0.9	-1.6(-2.6,-0.6)	3.0(20)	0.3(-0.7,1.3)
Southern Sub-saharan Africa	0.9	-1.6(-2.3,-0.9)	5.9(18)	1.5(0.1,2.9)
North Africa / Middle East	0.8	2.5(1.7,3.2)	25.5(4)	1.5(0.7,2.3)
Tropical Latin America	0.6	-3.0(-4.3,-1.7)	5.0(19)	0.2(-0.6,1.0)
Central Asia	0.6	0.5(-0.6,1.7)	17.3(6)	1.7(0.7,2.7)
Andean Latin America	0.6	-0.0(-2.1,2.0)	6.6(16)	1.4(-0.7,3.5)
South Asia	0.5	1.7(0.7,2.7)	34.6(2)	2.9(2.2,3.6)
Southeast Asia	0.5	-0.1(-1.0,0.8)	11.0(11)	2.7(1.9,3.5)
Caribbean	0.2	-0.8(-2.2,0.6)	7.0(15)	-0.3(-1.3,0.7)
West Sub-saharan Africa	0.2	-0.4(-1.5,0.7)	30.8(3)	-0.1(-1.0,0.8)
Central Sub-saharan Africa	0.1	-1.7(-2.7,-0.8)	11.4(10)	-0.4(-1.2,0.4)
East Sub-saharan Africa	0.1	-0.3(-2.1,1.4)	9.8(13)	1.0(0.1,1.9)
Oceania	<0.1	-0.4(-2.1,1.4)	2.3(21)	3.9(2.6,5.2)
GLOBAL	**1.7**	**1.0(0.74,1.3)**	**26.4**	**2.1(1.6,2.6)**

Figure Legends

Figure 1: Long-term (1996-2012) mean satellite-derived ground-level NO_2 concentrations (top), and trends in NO_2 over the same period (bottom). Numbered regions and their boundaries correspond to the region names and numbers given in Table 1.

Figure 2: Annual mean satellite-derived (solid blue lines) and ground-based (dashed lines) NO_2 concentrations over North American and European urban areas, normalized to respective long-term means. "N" denotes the number of ground-based stations within the urban area. Linear trends are reported as % yr^{-1} with 95% confidence intervals. Error bars denote the standard error of the annual ground-based measurements or the standard error of satellite pixels within the area.

Figure 3: Maps (with regional boundaries) of mean satellite-derived NO_2 concentrations at the beginning and end of the record for the four regions with the highest long-term population-weighted mean NO_2: North America (top), Western Europe (middle), and East China and Asia Pacific (bottom). Time series of annual population-weighted mean NO_2 for these regions are shown in the right panel, with the 1996-2012 linear slopes reported as % yr^{-1} (relative to the long term mean), and 95% confidence intervals. The slope from 2004-2010 for North America (relative to the long term mean) is also shown below the long-term trend.

Figure 4: Population and satellite-derived ground-level NO_2 plotted as cumulative distribution plots for the same four regions depicted in Figure 3.

Figure 1.

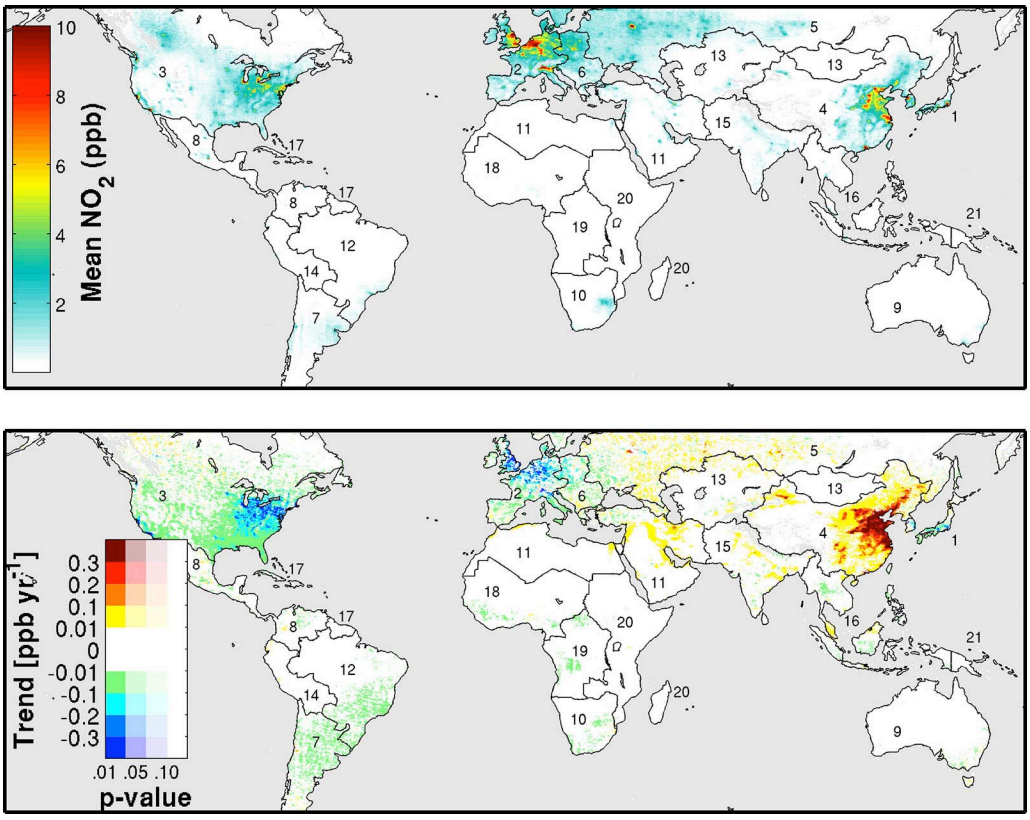
Mean NO_2 (ppb)
10
8
6
4
2
Trend [ppb yr^{-1}]
0.3
0.2
0.1
0.01
0
-0.01
-0.1
-0.2
-0.3
.01 .05 .10
p-value

Figure 2.

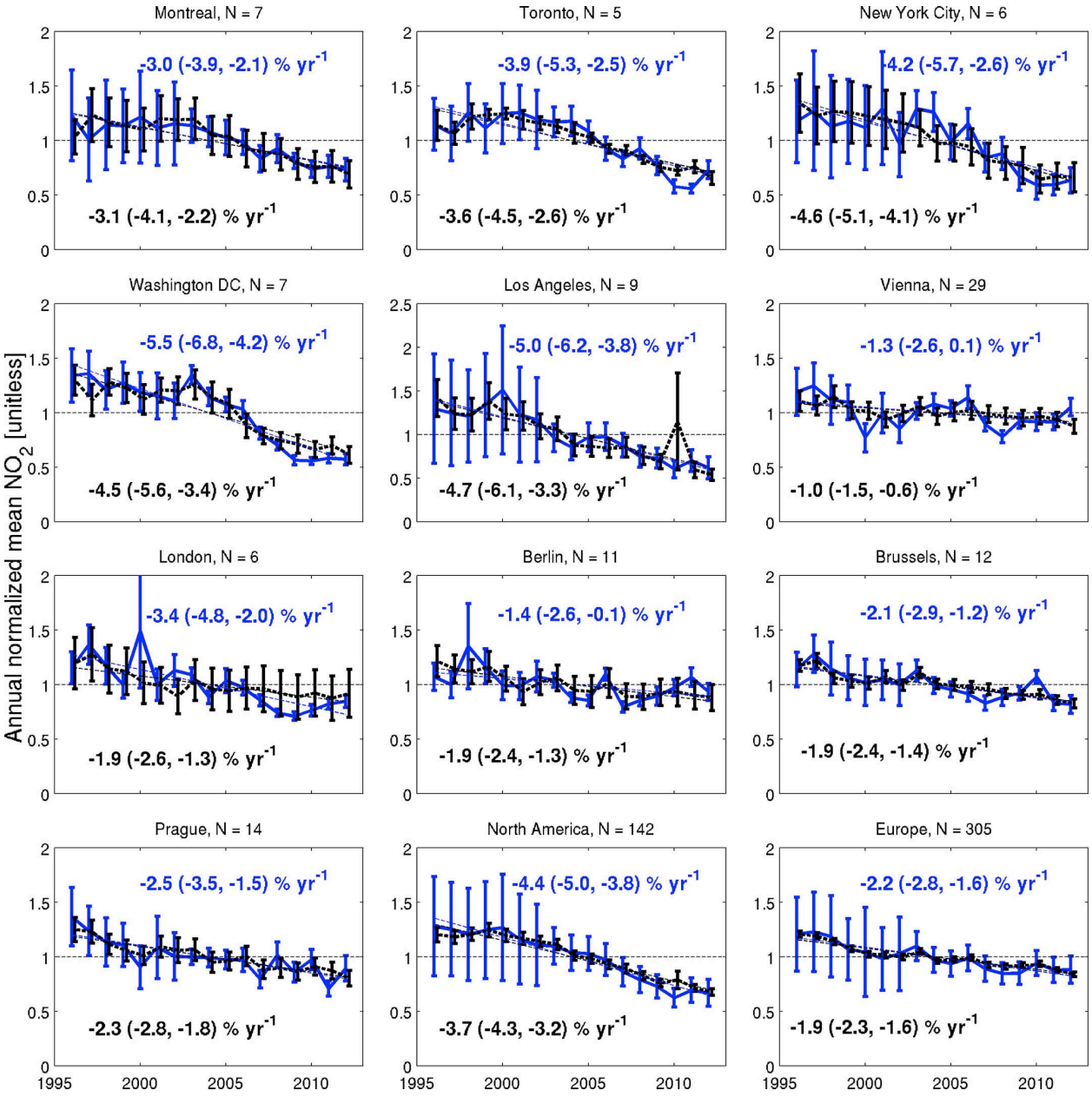
Montreal, N = 7
-3.0 (-3.9, -2.1) % yr-1
-3.1 (-4.1, -2.2) % yr-1
Toronto, N = 5
-3.9 (-5.3, -2.5) % yr-1
-3.6 (-4.5, -2.6) % yr-1
New York City, N = 6
-4.2 (-5.7, -2.6) % yr-1
-4.6 (-5.1, -4.1) % yr-1
Washington DC, N = 7
-5.5 (-6.8, -4.2) % yr-1
-4.5 (-5.6, -3.4) % yr-1
Los Angeles, N = 9
-5.0 (-6.2, -3.8) % yr-1
-4.7 (-6.1, -3.3) % yr-1
Vienna, N = 29
-1.3 (-2.6, 0.1) % yr-1
-1.0 (-1.5, -0.6) % yr-1
London, N = 6
-3.4 (-4.8, -2.0) % yr-1
-1.9 (-2.6, -1.3) % yr-1
Berlin, N = 11
-1.4 (-2.6, -0.1) % yr-1
-1.9 (-2.4, -1.3) % yr-1
Brussels, N = 12
-2.1 (-2.9, -1.2) % yr-1
-1.9 (-2.4, -1.4) % yr-1
Prague, N = 14
-2.5 (-3.5, -1.5) % yr-1
-2.3 (-2.8, -1.8) % yr-1
North America, N = 142
-4.4 (-5.0, -3.8) % yr-1
-3.7 (-4.3, -3.2) % yr-1
Europe, N = 305
-2.2 (-2.8, -1.6) % yr-1
-1.9 (-2.3, -1.6) % yr-1
Annual normalized mean NO2 [unitless]
1995
2000
2005
2010

Figure 3.

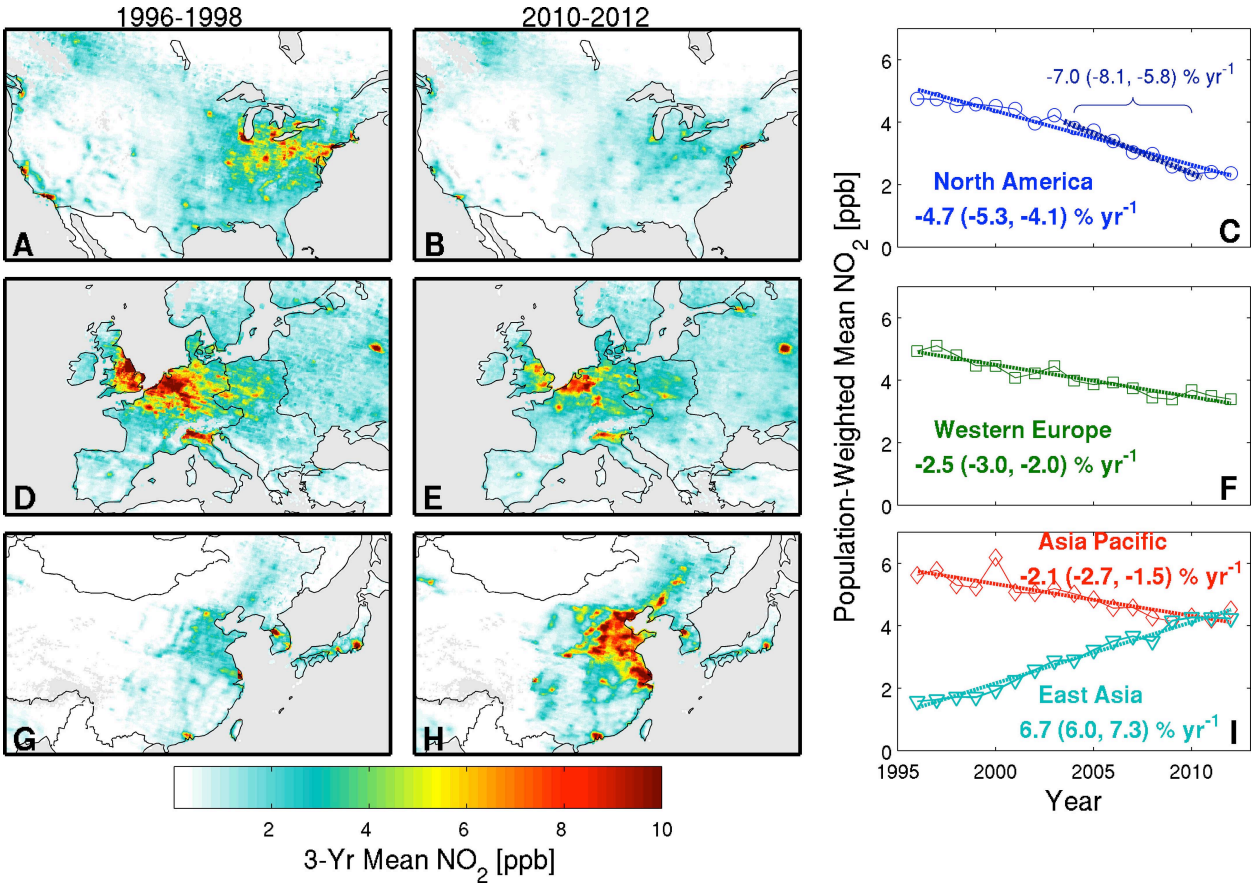
1996-1998
2010-2012
A
B
D
E
G
H
2
4
6
8
10
3-Yr Mean NO2 [ppb]
-7.0 (-8.1, -5.8) % yr-1
North America
-4.7 (-5.3, -4.1) % yr-1
C
Western Europe
-2.5 (-3.0, -2.0) % yr-1
F
Asia Pacific
-2.1 (-2.7, -1.5) % yr-1
East Asia
6.7 (6.0, 7.3) % yr-1
I
Population-Weighted Mean NO2 [ppb]
0
2
4
6
1995
2000
2005
2010
Year

Figure 4.

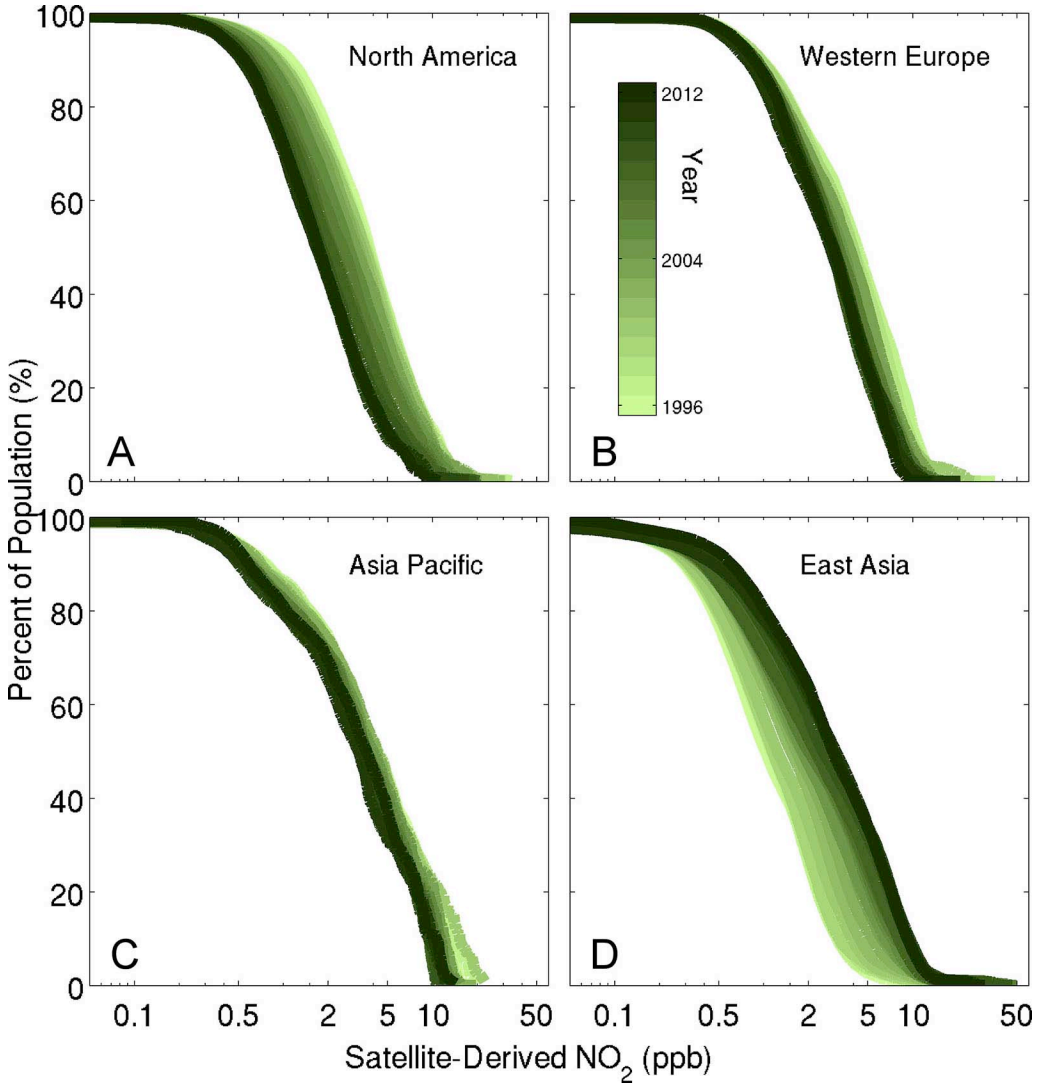
North America
Western Europe
Asia Pacific
East Asia
A
B
C
D
2012
Year
2004
1996
Percent of Population (%)
Satellite-Derived NO2 (ppb)
0
20
40
60
80
100
0.1
0.5
2
5
10
50